Materials Research Proceedings **26** (2023) 189-194 https://doi.org/10.21741/9781644902431-31

Dynamic performance of an aerostatic pad with internal pressure control

Federico Colombo[1, a], Luigi Lentini[1,b*], Terenziano Raparelli[1,c] and Andrea Trivella[1,d]

[1] Politecnico di Torino, DIMEAS department, Italy

[a]federico.colombo@polito.it, [b]luigi.lentini@polito.it, [c]terenziano.raparelli@polito.it, [d]andrea.trivella@polito.it

Keywords: Compensation, Diaphragm Valve, Aerostatic Bearings, Infinite Stiffness

Abstract. This paper presents a theoretical study on the dynamic performance of an aerostatic pad with an internal pressure control. The trend of the dynamic stiffness and damping over the frequency domain is analysed.

Introduction

Thanks to their zero friction, cleanness and infinite life, aerostatic pads are widely used in high-precision applications, e.g., machine tools, measuring machines and power board testing [1]. However, due to the compressibility of the lubricant, aerostatic bearings are characterized by relative low stiffness and poor damping. Much effort has been done in order to compensate for these drawbacks. A suitable selection and optimization of the feeding system of air pads is a common solution that makes it possible to obtain limited performance improvements. Several authors investigated to what extent the dimension, location and number of orifices affect aerostatic pad performance [2]. Compound restrictors, i.e., machining shallow grooves on the active surface of the pad, increase load capacity and stiffness but significantly reduce the bearing damping [3, 4]. The use of porous surfaces [5] is another solution that lead to performance improvement but it presents critical issues related to the choice of material that should have both suitable porosity and impact toughness.

Passive and active compensation methods makes it possible to significantly increase the static and dynamic performance of aerostatic bearings. In passive compensation methods bearings are integrated with devices that exploit only the energy associated with the supply pressure, e.g., pneumatic regulating valves and compliant elements. Conversely, actively compensated bearings are integrated with elements such as sensors, controllers and actuators that require external sources of energy to function. Active bearings have excellent static and dynamic performance [6–8] but the solutions are quite expensive. By contrast passive compensation solutions, notwithstanding their lower dynamics and effectiveness, represent an acceptable and cheap alternative to be integrated into current industrial applications [9]. In order to simplify the setting of the passive compensation, in work [10] the control signal and the supply pressure of the regulating valve are not dependent; the static behavior of the controlled pad is theoretically and experimentally analysed.

In this work the dynamic behavior of the system presented in [10] is theoretically analysed, evaluating the stiffness and damping of the air gap as the frequency of a sinusoidal load applied to the bearing varies. The numerical study is carried out by using a suitable lumped parameter model.

The compensated air pad

Figure 1 shows the geometry of the aerostatic pad considered in this numerical investigation. It has a rectangular base of 110x50 mm^2 and presents four supply holes with a diameter $d_p = 0.5$

Materials Research Proceedings **26** (2023) 189-194 https://doi.org/10.21741/9781644902431-31

mm which are located in the middle of a grooved rectangular supply line of dimensions 80x30 mm^2. These grooves have a triangular cross-section of depth h_g=60 μm and base w_g=0.3 mm.

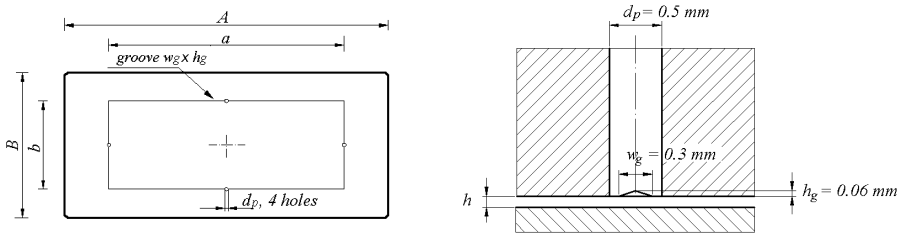

Fig. 1. The geometry of the aerostatic pad.

Figure 2a shows the scheme of the differential diaphragm valve that has been integrated with the aerostatic pad. The nozzle (1) has a diameter d_n= 0.5 mm and it is located in the chamber (2) that along with the chamber (3) is supplied with a constant supply pressure p_s. The other chambers (3) and (4) are supplied with a feedback $P_{Feedback}$ and a reference P_{Ref} pressures and they are separated through diaphragms (5 and 6) with different dimensions. The feedback pressure depends on the operating conditions of the pad (supply pressure and air gap height) and it is measured by means of back-pressure hole of diameter d_3=0.25 mm that is located on the active surface of the pad. The air flow supplied to the pad depends on the position of the shutter (7) that in turn depends on the difference between the feedback and supply pressure along with the diaphragm stiffnesses k_v.

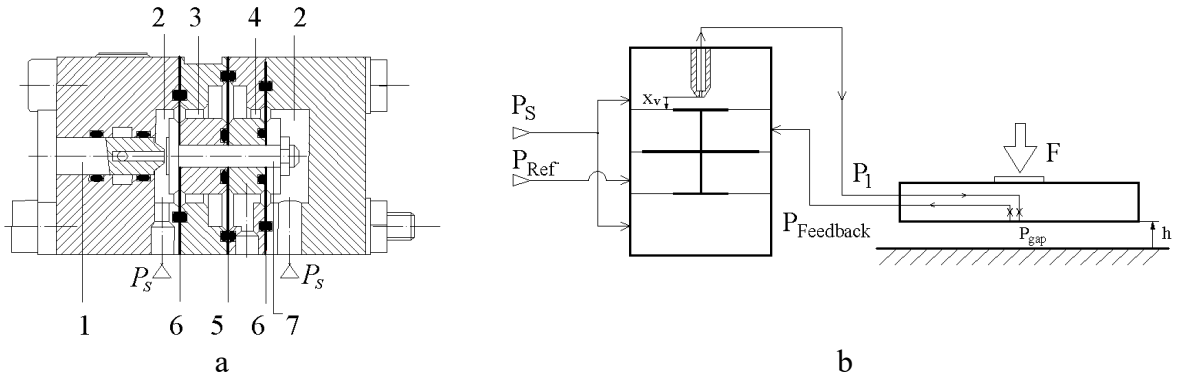

Fig. 2. a) scheme of the differential diaphragm valve. b) functional scheme of the control system.

Figure 2b shows a scheme useful to clarify the functioning of the system. Once the pressure P_S and P_{Ref} and the initial nozzle-shutter distance x_v are defined, the valve suitably regulates the air flow supplied to the pad depending on the applied load F. When the load increases, the pressures P_{gap} and $P_{Feedback}$ increase too producing a downward displacement of the shutter and in turn an increase of the air flow supplied to the pad. Consequently, the increase of the air flow produces an increase of the air gap height h that partially or completely compensated for the load variation. Conversely, the opposite holds in the presence of load reductions.

The numerical model

The considered compensated pad is modelled through a lumped parameter model consisting of pneumatic capacitances and resistances. Figure 3 shows the pneumatic model of the system.

Materials Research Proceedings **26** (2023) 189-194 https://doi.org/10.21741/9781644902431-31

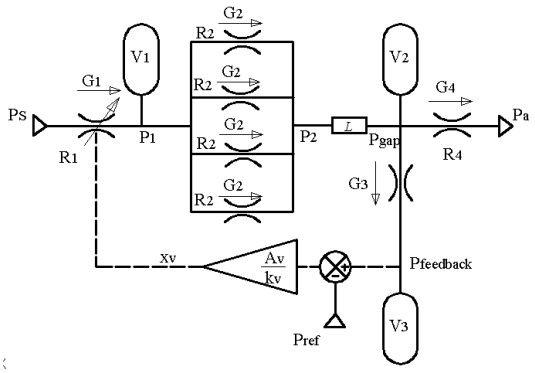

Fig. 3. Pneumatic model of the control system.

The nozzle and the air gap height are modelled through the variable pneumatic resistances R_1 and R_4, whereas the supply and back pressure hole of the pad are modelled through the constant resistances, R_2 and R_3 respectively. The air gap pressure (P_{gap}) distribution is considered uniform within the rectangle defined by the grooves (a x b) and linear in the region outside it. V_1, and V_3 are the volumes related to the ducts of the valve and the pad, whereas $V_2 = abh+V_g$ is the sum of the air gap and groove volume. The nozzle-shutter distance x_v is defined on the basis of the following equation:

$$\begin{cases} x_v = x_{by-pass} & x_v \leq x_{by-pass} \\ x_v = x_0 + A_v \frac{(P_{feedback} - P_{Ref})}{k_v} & x_v > x_{by-pass} \end{cases} \tag{1}$$

where $x_{by-pass}$ is a threshold takes into account the air leakages experienced when the shutter is in contact with the nozzle (40 μm); x_0 is the initial distance between the nozzle and the shutter it is defined when $P_{feedback}$ and P_{Ref} are equal. A_v is the effective area of the valve diaphragms where the feedback and reference pressure are applied. The air mass flow rates passing through the resistances R_1, R_2, R_3 are modelled through the ISO formula 6358:

$$G_i = K_T \, cd_i \, \frac{0.685}{\sqrt{R\,T}} \, A_i P_{up} \sqrt{1 - \left(\frac{\frac{P_{down}}{P_{up}} - b_c}{1 - b_c} \right)^2} \tag{2}$$

where K_T is the square root of the ratio between the valve (293 K) and the reference absolute temperatures (273 K). A_i, cd_i, P_{up} and $P_{down}$are the annular area, discharge coefficient and the upstream and downstream pressures of the ith lumped resistance (i = 1, 2, 3); b_c=0.528 is the theoretical critical pressure ratio assuming an isentropic expansion. The discharge coefficients are assumed to be functions of the Reynolds' Number Re_i related to the flow of each resistance:

$$\begin{aligned} & cd_i = 1.05(1 - 0.3\, e^{-0.005\, Re_i}) \\ & Re_1 = \frac{G_1}{\pi \mu d_1}; \;\; Re_2 = \frac{G_2\, h}{\mu A_2}; \;\; Re_3 = \frac{G_3}{\pi \mu d_3}; \; A_2 = \pi d_p h + w_g h_g \; ; \; d_1 = d_n \end{aligned} \tag{3}$$

Where $\mu = 18.89 \cdot 10^{-6}$ Pa s is the dynamic air viscosity. The mass flow rates G_4 exhausted from the air gap under isothermal conditions is:

Materials Research Proceedings **26** (2023) 189-194 https://doi.org/10.21741/9781644902431-31

$$G_4 = \frac{1}{6\mu RT}\left(\frac{b}{A-a}+\frac{a}{B-b}\right)\left(P_{gap}^2 - P_a^2\right)h^3 \quad (4)$$

Where R, T are the constant of gas ($R = 287.1$ J/(kg K)) and the absolute ambient temperature ($T = 293$ K). The pad's dimensions *A*, *B*, *a*, *b* are shown in figure 1. P_a is the ambient pressure, P_{gap} is the equivalent uniform pressure expressed by an empirical formula adopted for this air pad geometry [11]:

$$P_{gap} = L\,(h, P_2) = \left[1 - 0.02^{\left(\frac{5}{h}\right)}\right]\cdot(P_2 - P_a) + P_a \quad (5)$$

where h is expressed in μm. The load capacity of the pad is computed by integration of the pressure distribution on its area:

$$F_p = \left[ab + AB + \frac{(Ab+aB)}{2}\right]\frac{(P_{gap}-P_a)}{3} \quad (6)$$

The continuity equations related to the incoming and outgoing mass flow rates for each volume V_1, V_2, V_3 and to the corresponding pressures $P_1, P_{gap}, P_{feedback}$ are:

$$G_1 - 4G_2 = \frac{V_1}{RT}\frac{dP_1}{dt}$$

$$4G_2 - G_4 - G_3 = \frac{P_{gap}ab}{RT}\frac{dh}{dt} + \frac{V_2}{RT}\frac{dP_{gap}}{dt} \quad (7)$$

$$G_3 = \frac{V_3}{RT}\frac{dP_{feedback}}{dt}$$

The equilibrium equation of the pad (considered as a single degree of freedom system) is:

$$F - \mathrm{F}_P + M\frac{\mathrm{d}^2h}{dt^2} = 0 \quad (8)$$

where *F* is the vertical external load applied to the pad and *M* the mass related to the supported payload (*F*=*M*g).

Numerical results and Discussion

At the supply pressure $P_S = 0.5$ MPa the regulation parameters of the valve are identified with the numerical model: x_0= 55 μm, $P_{Ref} = P_{feedback} = 0.37$ MPa. In this way, the compensation works in a range of air gap near to h = 9.5 μm. The static behavior of the compensated air pad has been widely discussed in [10].

To determine the dynamic parameters *K* and *c* of the air bearing a sinusoidal load *F* of amplitude *ΔF* and frequency f is imposed around the initial point of static equilibrium. By applying a small amplitude load (*ΔF* is about 1% of the initial static load) it is possible to define with good accuracy the dynamic parameters of the air bearing at each air gap height. With the imposed sinusoidal load the air gap h is calculated and plotted as a function of the time; the amplitude *Δh* and the time delay *Δt* between the input signal *F* and the output signal h are therefore determined in stationary conditions. The pressure force of the air gap is the sum of the elastic component due to the stiffness

Materials Research Proceedings **26** (2023) 189-194 https://doi.org/10.21741/9781644902431-31

of the air gap and the viscous component due to the damping of the air gap. Considering all the acting forces as rotating vectors on a complex plane, the equilibrium of the forces decomposed in the direction of the elastic force and in the direction of the viscous force allows to obtain the values of K and c as a function of the frequency, according to the equations (9):

$$K(\omega) = \frac{\Delta F}{\Delta h}\cos(\phi) + M\omega^2 ; \quad c(\omega) = \frac{\Delta F}{\Delta h}\frac{\sin(\phi)}{\omega} \tag{9}$$

Where $\omega = 2\pi f$ is the angular frequency, $\phi = \omega \Delta t$ is the phase lag between the input and the output signals.

Figure 4 shows the trend of the dynamic stiffness K and the damping c over a frequency range from 0 to 30 Hz and considering initial static conditions near to h = 9.5 μm.

At low frequency, stiffness and damping of the air gap are much higher than those obtainable without the valve and they quickly reduce as ω increases. Outside the overcompensation zone, the stiffness is always positive, otherwise it can be positive or negative as a function of ω. Further studies will be involved to analyze the dynamic stability of the system, as already made for the solution studied in [12].

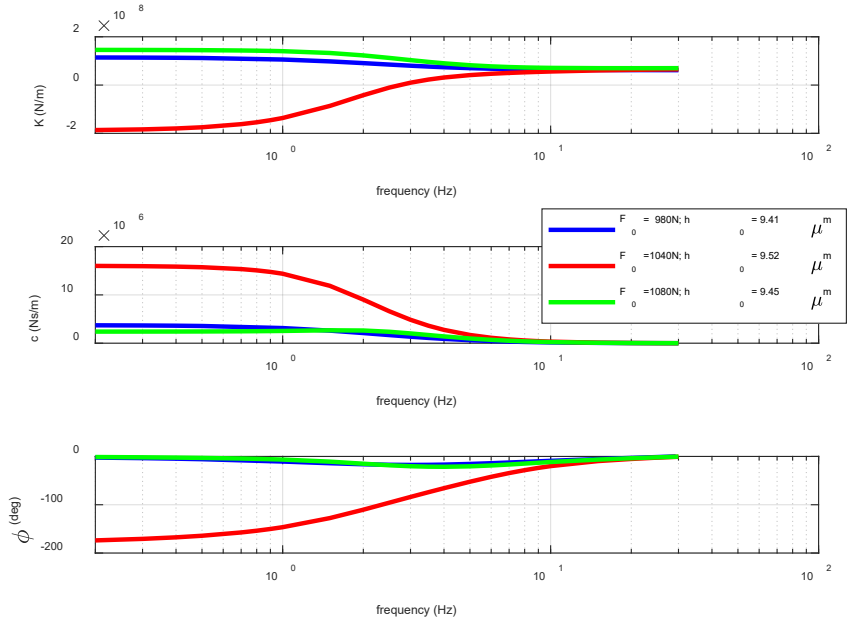

Fig. 4. Stiffness K, damping c and phase delay ϕ of the compensated air pad: numerical results. $P_S = 0.5\ MPa,\ k_v = 50\ N/mm,\ d_v = 0.5\ mm,\ d_P = 0.5\ mm.$

Conclusions

This paper presents a preliminary investigation on the dynamic performance of an aerostatic pad with internal pressure control. The dynamic performance of the compensated air pad dramatically decreases as the frequency increases due to the presence of the valve. For frequencies below about 40 Hz the phase lag is negative, which means the presence of the valve makes the displacement of the air pad in advance with respect to the applied external force. The results indicate that this compensation method represents an efficient and cost-effective method for low frequency air pad applications. Further studies will be aimed to compare numerical and experimental results and to analyze the stability of the proposed control system.

References

[1] Gao, Q., Chen, W., Lu, L., Huo, D., Cheng, K.: Aerostatic bearings design and analysis with the application to precision engineering: State-of-the-art and future perspectives. Trib. Intern. 139, (2019), 1-17. https://doi.org/10.1016/j.triboint.2019.02.020

[2] Charki, A., Diop, K., Champmartin, S., Ambari, A.: Numerical simulation and experimental study of thrust air bearings with multiple orifices. International Journal of Mechanical Sciences. 72, (2013), 28–38. https://doi.org/10.1016/j.ijmecsci.2013.03.006

[3] Ma, W., Cui, J., Liu, Y., Tan, J.: Improving the pneumatic hammer stability of aero-static thrust bearing with recess using damping orifices. Trib. Intern. 103, (2016), 281–288. https://doi.org/10.1016/j.triboint.2016.06.009

[4] Yoshimoto, S., Tamura, J., Nakamura, T.: Dynamic tilt characteristics of aerostatic rectangular double-pad thrust bearings with compound restrictors. Trib. Intern. 32, (1999), 731–738. https://doi.org/10.1016/S0301-679X(00)00004-9

[5] Kwan, Y.B.P., Corbett, J.: Porous aerostatic bearings: an updated review. Wear 222, 1998, 69–73. https://doi.org/10.1016/S0043-1648(98)00285-3

[6] Al-Bender, F.: On the modelling of the dynamic characteristics of aerostatic bearing films: From stability analysis to active compensation. Precision Engineering. 33, (2009), 117–126. https://doi.org/10.1016/j.precisioneng.2008.06.003

[7] Maamari, N., Krebs, A., Weikert, S., Wegener, K.: Centrally fed orifice based active aerostatic bearing with quasi-infinite static stiffness and high servo compliance. Trib. Intern. 129, (2019), 297–313. https://doi.org/10.1016/j.triboint.2018.08.024

[8] Colombo, F., Lentini, L., Raparelli, T., Viktorov, V.: Actively compensated aerostatic thrust bearing: design, modelling and experimental validation. Meccanica, 52, (2017), 1–16. https://doi.org/10.1007/s11012-017-0689-y

[9] Ghodsiyeh, D., Colombo, F., Lentini, L., Raparelli, T., Trivella, A., Viktorov, V.: An infinite stiffness aerostatic pad with a diaphragm valve. Tribology International. 141, (2020), 105964. https://doi.org/10.1016/j.triboint.2019.105964

[10] Lentini, L., Colombo, F., Raparelli, T., Trivella, A., Viktorov, V.: An aerostatic pad with an internal pressure control. E3S Web Conferences. 197, (2020), 07002. https://doi.org/10.1051/e3sconf/202019707002

[11] Colombo, F., Lentini, L., Raparelli, T., Trivella, A., Viktorov, V.: A Lumped Model for Grooved Aerostatic Pad. Advances in Service and Industrial Robotics. Springer (2019), 678–686. https://doi.org/10.1007/978-3-030-00232-9_71

[12] Colombo, F., Lentini, L., Raparelli, T., Trivella, A., Viktorov, V.: Dynamic behaviour and stability analysis of a compensated aerostatic pad. 76th Italian National Congress ATI, 15-17 Settembre 2021. https://doi.org/10.1051/e3sconf/202131205003